Convection in Polymeric Fluids Subjected to Vertical Temperature Gradients

Minqin Li, Shengqing Xu, and Eugenia Kumacheva*

Department of Chemistry, University of Toronto, 80 St. George, Toronto, Ontario, M5S 3H6 Canada

Received December 27, 1999; Revised Manuscript Received April 4, 2000

ABSTRACT: We present a study of convection in thin layers of poly(dimethyl siloxane) (PDMS) oligomers end-terminated with different functional groups. In PDMS, silanol-, and aminopropyl-terminated PDMS, surface-tension-driven convection produces ordered hexagonal patterns with a critical wavenumber k ≈ 2. The onset of convection is close to that predicted by a linear theory. In thin films of methacryloxypropyl-terminated PDMS (MAOP-PDMS) surface-tension-driven convection is suppressed, despite the fact that macroscopic physical properties favor this type of convection. In thick films of MAOP-PDMS, mixed surface-tension- and buoyancy-driven convection occurs, generating hexagonal and roll-like patterns. We demonstrate that ordered nonequilibrium patterns induced in the fluid MAOP-PDMS films can be trapped in the solid state by photopolymerization.

Introduction

In recent years, spatial−temporal patterns in polymeric fluids have attracted much attention for at least two reasons.[1−7] First, polymer liquids as complex fluids provide a rich phenomenology in nonequilibrium structures due to coupling of thermodynamic and kinetic effects. Second, in contrast to simple fluids, patterns in polymeric or polymerizable fluids can be trapped in the solid state by solvent evaporation, polymerization, cross-linking, or gelation. Vitrified patterns can then be used in studies of nonequilibrium structures generated in the liquid state or, more importantly, can be employed for producing materials with unique properties and morphologies.

When a fluid polymeric film is subjected to a vertical temperature gradient and a threshold of instability is exceeded, surface-tension-driven and/or buoyancy-driven convection occurs in the layer, producing two-dimensional patterns with a high degree of order and symmetry.[8] In simple fluids, convection patterns dissipate when the temperature difference across the film diminishes and the system returns to a conductive regime. By contrast, in polymeric fluids, ordered convection patterns can be vitrified in at least two cases. First, in liquid films cast from polymer solutions, solvent evaporation induces vertical temperature gradients. Convection patterns appear at a particular solvent evaporation rate and "freeze" when a system undergoes a glass transition.[3,4,6] Second, in solvent-free films of monomers or oligomers, vertical temperature gradients can be produced in a rather standard way by heating the bottom and cooling the top of the liquid film. After convection generates a pattern with a desired planform, the latter can be kinetically trapped by polymerization. In these systems the limiting parameter is the viscosity of the fluid, since in high viscous fluids convection is suppressed (see below).

Recently, we have shown how ordered convection patterns can be produced and vitrified in films cast from polymer solutions.[4] In the present paper, we address the second approach; i.e., we demonstrate how ordered two-dimensional patterns can be generated and vitrified in a *single*-component fluid using UV-induced polymerization. The second objective of this work is to examine to what extent the difference in the chemical composition of PDMS fluids affects the formation of the convection patterns.

Background

Convection in thin fluid layers of simple fluids has been extensively studied both experimentally and theoretically.[8] Here we briefly outline the main features of surface-tension-driven and buoyancy-driven convection, which are essential for the interpretation of experimental results presented in the current work.

Surface-tension-driven convection (Bénard−Marangoni convection) results from the temperature-dependent surface tension gradients in thin fluid layers. The balance between the surface-tension-governed forces favoring convection and the dissipation resulting from viscous friction and thermodiffusion is expressed by the dimensionless Marangoni number

$$\mathrm{Ma} = [-(\mathrm{d}\gamma/\mathrm{dT})\Delta\mathrm{T}d]/\rho\nu k \qquad (1)$$

where d is the thickness of the film, γ, ρ, k, and ν are the fluid surface tension, density, thermal diffusivity, and kinematic viscosity, respectively, $\nu = \eta/\rho$, η is the dynamic viscosity, and ΔT is the difference in temperature between the bottom and the top surfaces of the layer. Linear theory[9] yields the onset of convection at $Ma_c \approx 80$, which is in accord with experimental observations.[10] In single-component simple fluids above the onset of instability Bénard−Marangoni convection generally produces hexagonal patterns with a mean wavenumber $\mathrm{k} = 4\pi\mathrm{d}/\sqrt{3}\lambda$ where λ is the characteristic length of the pattern.

Buoyancy-driven convection (Rayleigh−Bénard convection) originates from the temperature-dependent gradients in the density of the fluid and is described by the Rayleigh number

$$\mathrm{Ra} = \mathrm{g}\beta\Delta\mathrm{T}d^3/\nu k \qquad (2)$$

where β is the thermal volume expansion coefficient and g is the acceleration of gravity.

For fluid films with a free upper surface the critical Rayleigh number, $Ra_c \approx 669$.[11] Typical structures obtained in this type of convection are roll-like patterns.

10.1021/ma992156t CCC: $19.00
Published on Web 06/08/2000

Table 1. Properties of PDMS Fluids Used in Convection Experiments[13]

fluid	mol wt (g/mol)	end-terminated group content (%)	kinematic viscosity at $T = 25$ °C (cSt)	density at $T = 25$ °C (g/cm^3)	thermal expansion (°C^{-1})
PDMS	2000		20	0.950	0.00107
NH_2-PDMS	950	3.0−3.2	37	0.980	
OH-PDMS	550	4.0−6.0	23	0.950	
MAOP-PDMS	386			0.980	

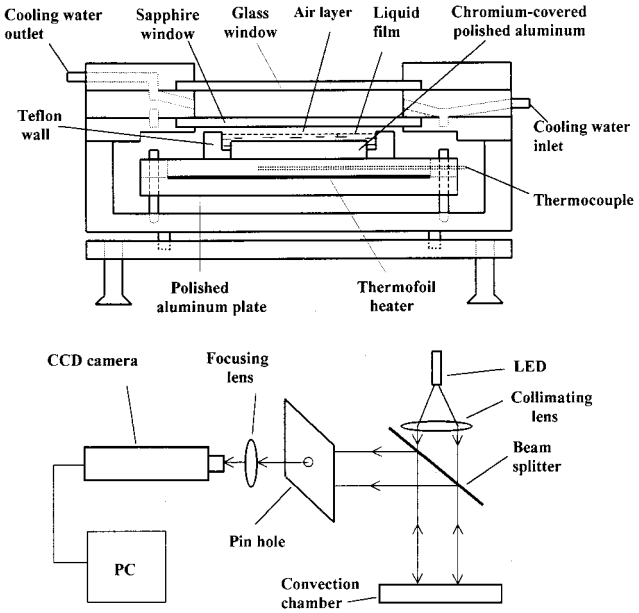

Figure 1. Experimental setup for convection studies: (a, top) assembly of the convection chamber; (b, bottom) schematics of the shadowgraph optics assembly.

Since Ra ∝ d^3 and Ma ∝ d, buoyancy-generated convection dominates in thick films, whereas for films thinner than ca. 1 mm, Ma > Ra and convection is governed by the surface-tension gradients.

In moderately thick films with d about several millimeters both surface-tension and buoyancy forces contribute to convection, and the threshold values of Ra and Ma are no longer independent. The condition of instability in the film is determined as[12]

$$\mathrm{Ra}/Ra_c + \mathrm{Ma}/Ma_c = 1 \qquad (3)$$

and the temperature threshold of convection, ΔT_c, can be calculated as

$$\Delta T_c = (\nu k)\{[(\mathrm{d}\gamma/\mathrm{d}T)d]/(Ma_c\rho)] + g\beta \mathrm{d}^3/Ra_c]\}^{-1} \qquad (4)$$

Experimental Section

Poly(dimethylsiloxane) (PDMS) and PDMS oligomers terminated at both ends with aminopropyl, silanol, and methacryloxypropyl groups are designated in this work as NH_2-PDMS, OH-PDMS, and MAOP-PDMS, respectively. All samples were purchased from Gelest, Inc. Prior to the convection experiments all liquids were maintained under reduced pressure for a week to remove traces of volatile solvents. The properties of the oligomers are given in Table 1.[13] 1-Hydroxycyclohexyl phenyl ketone (Aldrich) was used as a photoinitiator for photopolymerization of MAOP-PDMS.

Convection patterns were visualized using a shadowgraph technique. Figure 1a shows schematically the experimental setup. A fluid oligomer layer with a thickness varying from ca. 0.1 to ca. 0.3 cm was placed onto a polished aluminum plate coated with a 1 μm thick layer of chromium. The diameter of the aluminum mirror was 5.0 ± 0.005 cm; i.e., the aspect ratio Γ in the convection experiments varied from 50 to 17. The thickness of the layer was determined with the accuracy of ±0.002 cm by measuring precisely the volume of the liquid induced in the apparatus and the area of the plate. The top surface of the liquid layer was bounded by a uniform layer of air with a thickness d_a varying from 0.1 to 0.2 cm.

The bottom surface of the film was uniformly heated using a thin-layer electric heater. The temperature of the heater was controlled to ±0.1 °C using a Brookfield temperature controller (model 74R). For each experimental point the system was equilibrated for at least 1 h.

The free surface of the liquid film was cooled through the air layer by purging cooling water between the sapphire and the glass windows. The temperature of the water was held constant at 20.0 ± 0.1 °C using a temperature-controlled circulator (M3 Lauda).

The temperature difference across the fluid film was calculated assuming conductive heat transport as[14]

$$\Delta T = (T_b - T_w)/[1 + (d_a k_l)/(d k_a)] \qquad (5)$$

where T_b is the temperature of the aluminum plate (assumed to be equal to the temperature of the bottom surface of the liquid film), T_w is the temperature of the cooling water, d_a and d are the thicknesses of the air gap and the fluid film, respectively, and k_a and k_l are the thermal conductivities of air and the fluid, respectively. $k_a = 2.55 \times 10^3$ erg/(cm s °C)[15] and $k_l = 1.25 \times 10^4$erg/(cm s °C).[10] The value of ΔT varied from 0.01 to ΔT = 8.49 °C.

The apparatus was leveled to eliminate variations in the thickness of the fluid films. The distance between the metal plate and the sapphire window was controlled with an accuracy of ±0.005 mm using shims (Lawton Industries, Inc.).

A beam of light produced by an ultrabright light-emitting diode (LED) (Electro Sonic Canada) was shone through the liquid layer (Figure 1b), reflected from the chromium-covered plate, passed through the beam splitter, and captured by a CCD camera (Pulnex TM 40) linked with a computer-controlled frame grabber and a time-lapse VCR. The contrast in the image appeared due to the local refractive index variations in the liquid layer. Image analysis was carried out using Image Tool software (Health Science Center, University of Texas, San Antonio, TX).

Convection patterns induced in the MAOP-PDMS films were trapped in a solid state by polymerization of the fluid using a high-intensity UV cure unit Uvaprint 40C/CE.

The temperature dependence of the surface tension of the fluids studied in this work was measured using a DuNouy tensiometer (CSC Scientific Company, Inc.). The temperature dependence of viscosity was measured using an Ubbelhode viscometer (flow constant K = 0.010 35 cSt/s). The dependence of viscosity of MAOP-PDMS on the shear rate was studied using Brookfield viscometer (Brookfield Engineering Laboratory Inc.). The thermodiffusivity of MAOP-PDMS was measured using a thermal-wave resonator technique.[16]

Results and Discussion

Experiments were carried out by slowly heating the aluminum plate to a particular temperature and observing patterns emerging at the air−liquid interface. Figure 2 shows typical convection patterns induced in 0.1376 cm thick films of PDMS, NH_2-PDMS, and OH-PDMS. The first evidence of convection appeared when the value of ΔT exceeded the critical value of ΔT_c characteristic for each oligomer, i.e., 1.52, 2.81, and 1.86

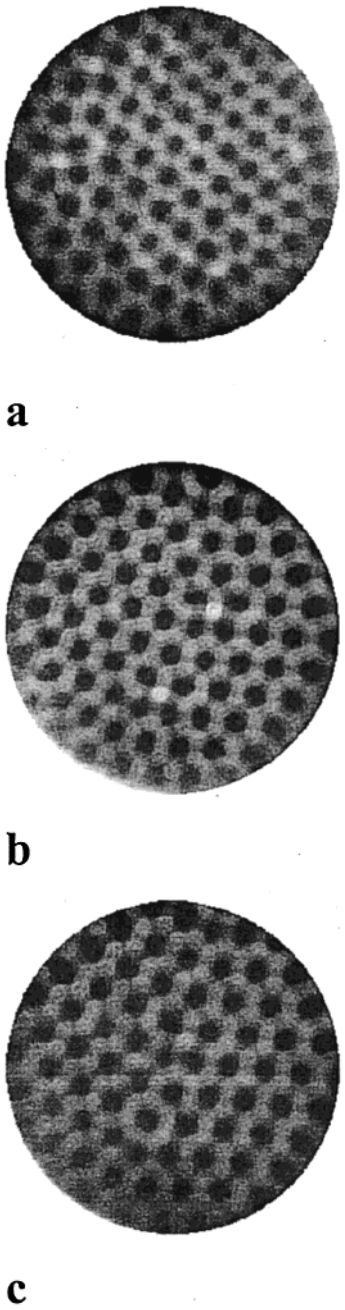

Figure 2. Typical convection patterns generated in 0.1376 cm thick oligomer films: (a) PDMS, $\Delta T = 2.06$ °C; (b) OH-PDMS, $\Delta T = 3.24$ °C; (c) NH_2-PDMS, $\Delta T = 2.33$ °C.

°C for PDMS, NH_2-PDMS, and OH-PDMS, respectively. Hexagonal planforms appeared at the onset ΔT persisted up to the maximum experimental $\Delta T = 6.02$ °C. The wavenumber k in all patterns increased slightly with the increasing vertical temperature gradients. The dependence was almost linear with $dk/d\epsilon \approx 0.09$ where $\epsilon = (\Delta T - \Delta T_c)/\Delta T_c$. Nevertheless, in the entire range of temperature gradients the periodicity of the hexagonal planforms remained on the order of several millimeters. No noticeable hysteresis was observed in pattern formation: upon heating and cooling of the liquid layer the convection patterns were almost identical.

To understand the origin of the difference in the onset of convection ΔT_c in PDMS, OH-PDMS, and NH_2-PDMS films, we studied the dependence of the surface tension

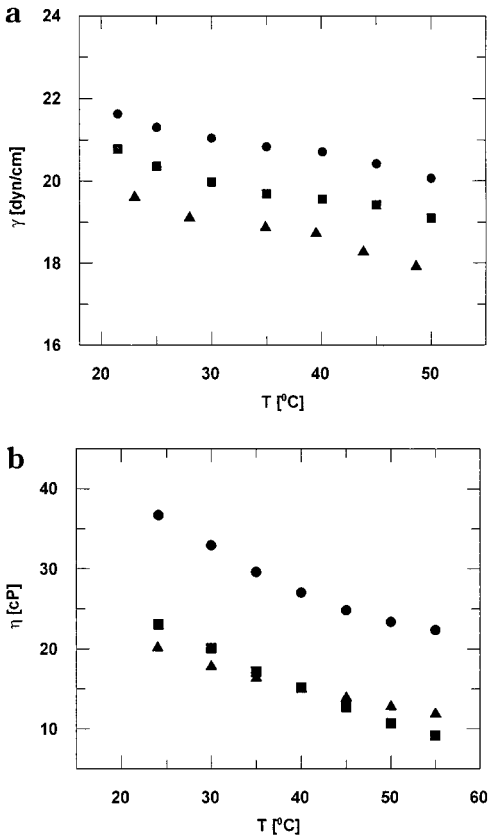

Figure 3. (a) Variation of surface tension with temperature for PDMS (▲), OH-PDMS (■), and NH_2-PDMS (●). (b) Variation of viscosity with temperature for PDMS (▲), OH-PDMS (■), and NH_2-PDMS (●).

Table 2. Critical Temperature Difference and Nondimensional Parameters of the Convection Patterns in PDMS, OH-PDMS, and NH_2-PDMS Films

fluid	d (cm)	ΔT_c (°C)	$-d\gamma/dT$ (dyn/cm)	η (cP)	Ma_c	k	pattern
PDMS	0.1376	1.52	0.063	18.6	88	1.98	hexagons
NH_2-PDMS	0.1376	2.81	0.050	28.5	88	1.96	hexagons
OH-PDMS	0.1376	1.86	0.054	20.5	84	1.99	hexagons

and viscosity of the oligomers on temperature.[17] Figure 3a shows the variation of the surface tension with temperature for PDMS, OH-PDMS, and NH_2-PDMS. In the temperature range varying from 21 to 50 °C the absolute values of the surface tension increased from PDMS to OH-PDMS and NH_2-PDMS. The values of $d\gamma/dT$ were −0.063, −0.054, and −0.050 dyn/(cm °C) for PDMS, OH-PDMS, and NH_2-PDMS, respectively.

Figure 3b shows the variation in viscosity of the oligomers for temperatures ranging from 24.5 to 55 °C. Both functionalized oligomers OH-PDMS and NH_2-PDMS feature a stronger decrease in viscosity upon heating than PDMS, which arises from a reduction of the average strength of the intermolecular hydrogen bonds at elevated temperatures. In addition, NH_2-PDMS has a substantially higher viscosity than OH-PDMS.

For all oligomers the variations of the surface tension and viscosity were reproduced in successive heating−cooling cycles.

In Table 2 the experimental values of ΔT_c, Ma_c,[18] and the mean wavenumber k are given for PDMS, OH-PDMS, and NH_2-PDMS oligomers. The values of Ma_c were calculated on the basis of the assumption that

viscosity gradually reduces from the bottom to the top of the liquid film. The average value of viscosity was used taken at $T = T_b - \Delta T/2$ from the profiles η vs T in Figure 3b. In all oligomeric films the threshold of convection is close to $Ma_c \approx 80$ predicted for the surface-tension-generated convection by the linear theory.[9] This could be anticipated, since the only parameter that could lead to a substantial change in convection is a decrease of oligomer viscosity upon heating. The reduction in viscosity in the experimental temperature range exceeding ΔT_c does not exceed 60% (Figure 3b). Such a change can still be considered as insufficient to invalidate the Boussinesq approximation,[19] in which all parameters except the surface tension are fixed.

Convection in MAOP-PDMS exhibited surprisingly different features. In films with $d = 0.1376$ cm, no convection was observed up to the maximum $\Delta T = 8.49$ °C. This was unexpected since the macroscopic physical parameters of MAOP-PDMS favor surface-tension driven convection, as will be discussed below. In thicker films, with $d = 0.2064$ cm a weak disordered bifurcation pattern appeared at $\Delta T_c = 5.19$ °C, which did not change significantly up to $\Delta T = 6.48$ °C. The most interesting pattern transformation following increase in ΔT was observed in MAOP-PDMS films with $d = 0.3096$ cm (Figure 4). The first weak pattern that had features of both hexagons and rolls was observed at $\Delta T = 3.66$ °C (Figure 4a). Following an increase in temperature, a mixed pattern gradually transformed through distorted rolls into perfectly symmetric rolls as shown in Figure 4b,c. While it was difficult to measure unambiguously the wavenumber in the mixed patterns, the value of k in the patterns dominated by rolls was 3.02 and did not change noticeably with the increase in ΔT.

To understand the origin of the difference between convection in MAOP-PDMS and other functionalized oligomers, we measured its viscosity, thermodiffusivity, and the dependence of the surface tension on temperature, i.e., the parameters that determine the value of Ma in eq 1. Figure 5 shows the dependence of the surface tension and viscosity of MAOP-PDMS on temperature for this material. In the entire temperature range the surface tension of MAOP-PDMS is substantially higher than that of PDMS, OH-PDMS, and NH_2-PDMS. However, the variation of the surface tension with temperature for MAOP-PDMS features a much stronger dependence than that for other oligomers with $d\gamma/dT = -0.11$ dyn/(cm °C).

The viscosity of the MAOP-PDMS samples at 22 °C was comparable with the viscosity of other oligomers; i.e., at 22 °C it is about 30% higher than the viscosity of PDMS and OH-PDMS and about 25 % lower than the viscosity of NH_2-PDMS. Upon heating MAOP-PDMS the decrease of its viscosity did not exceed 13%. The thermodiffusivity of MAOP-PDMS at 22 °C was measured to be 0.0086 cm^2/s. Thus, from eq 1 it could be expected that for the same value of $d = 0.1376$ cm the surface-tension-driven convection in the MAOP-PDMS films should appear at a *lower* value of ΔT_c than in PDMS, OH-PDMS, and NH_2-PDMS oligomers. However, our experiments indicated an opposite effect.

For thicker MAOP-PDMS films, in which both surface tension and buoyancy contribute to convection, the peculiarities of the latter can be expressed by a comparison of the experimental ΔT_c and the ΔT_c calculated from eq 4. These parameters are given in Table 3 for the MAOP-PDMS films with $d = 0.2064$ cm and $d = 0.3096$ cm. The experimental values of ΔT_c are substantially higher than calculated ΔT_c.

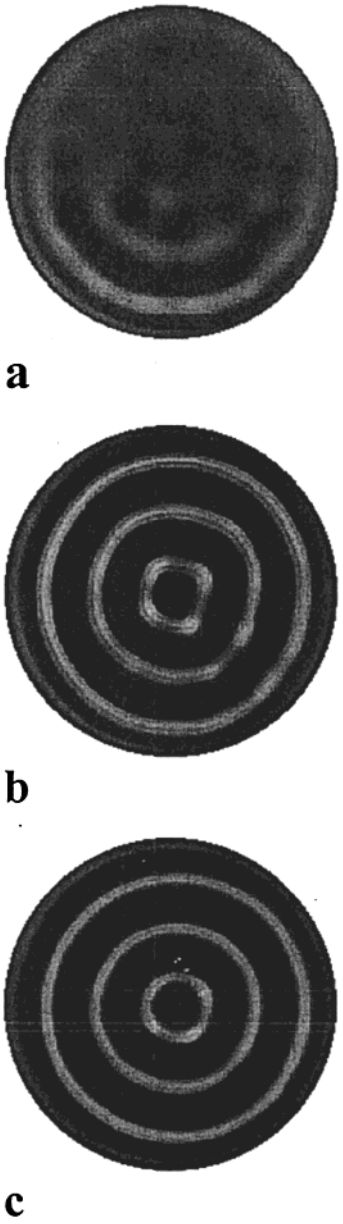

Figure 4. Evolution of convection patterns generated in MAOP-PDMS layers: (a) $\Delta T = 3.89$ °C, (b) $\Delta T = 5.03$ °C, and (c) $\Delta T = 6.81$ °C. $d = 0.3096$ mm.

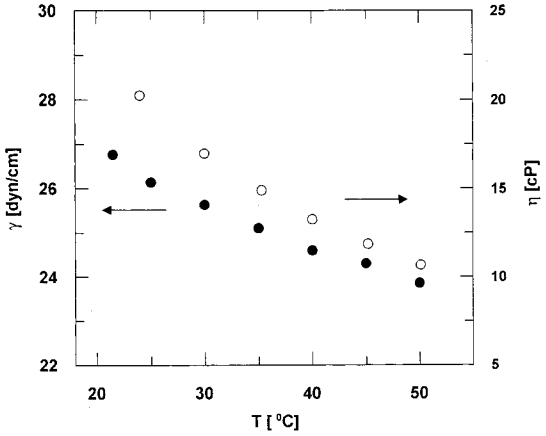

Figure 5. Temperature dependence of surface tension (●) and viscosity (○) of MAOP-PDMS.

Table 3. Critical Temperature Difference and Nondimensional Parameters of the Convection Patterns in MAOP-PDMS and MAOP-PDMS/HPK Films

fluid	d (cm)	ΔT_c (°C)	ΔT_c[a] (°C)	$-d\gamma/dT$ (dyn/cm °C)	η (cP)	k	pattern
	0.1376	8.49[b]		0.11	12.4		no convection
MAOP-PDMS	0.2064	5.19	0.38	0.11	12.0		weak disordered pattern
	0.3096	3.66	0.30	0.11	15.1		hexagons + rolls
	0.3096	5.14[c]		0.11	13.2	3.02	rolls
MAOP-PDMS/ HPK	0.3096	4.05	0.33	0.056	20.0		hexagons + rolls
	0.3096	5.78[c]		0.056	18.3	2.95	rolls

[a] The onset of convection estimated from eq 4. [b] The highest vertical temperature gradient achieved in convection experiment. [c] ΔT corresponding to transition to symmetric rolls.

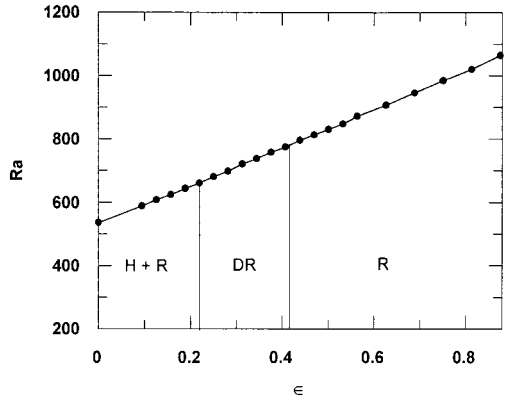

Figure 6. Stability diagram for convection patterns generated in MAOP-PDMS. $d = 0.3096$ cm. Mixed pattern of hexagons and rolls: H + R; distorted rolls: DR; perfect rolls: R.

A possible reason for the unusual convection properties of MAOP-PDMS could arise from its viscoelasticity or an " instantaneous elastic" response of the fluid.[20] For the low-molecular-weight MAOP-PDMS viscoelasticity could originate from the formation of a transient network via association of functional end groups. Measurements of the viscosity of MAOP-PDMS carried out in this work demonstrated Newtonian properties of the fluid for the shear rates varying from 0.65 to 64.68 s^{-1}; thus, viscoelasticity as a possible cause of the difference in behavior of MAOP-PDMS was ruled out.

At the moment we are unable to explain the origin of the suppressed Bènard−Marangoni convection in thin layers of MAOP-PDMS.

The stability diagram for the convection patterns in 0.3096 cm thick films of MAOP-PDMS is given in Figure 6 for the increasing $\epsilon = (\Delta T - \Delta T_c)/\Delta T_c$. The first evidence of mixed convection at $\epsilon = 0$ occurs at relatively high Ra. The absence of clear hexagons in the immediate vicinity of the instability threshold indicates that convection arises from both surface-tension gradients and buoyancy. Distorted rolls appear at $\epsilon = 0.22$, and at $\epsilon > 0.43$ concentric rolls become symmetric. Increase of ϵ to values higher than 0.87 does not result in any significant change of the convection patterns.

Convection patterns obtained at $\epsilon > 0.43$ were vitrified in a solid state by polymerization of MAOP-PDMS initiated by a small amount of the photoinitiator 1-hydroxycyclohexyl phenyl ketone (HPK). Prior to polymerization experiments, we examined to what extent the properties of liquid MAOP-PDMS change in the presence of HPK when the mixture is heated on time scales comparable with the those used in convection experiments.

Figure 7a shows the variation in viscosity of MAOP-PDMS in the presence of 1 wt % of the initiator. The profile of η vs T measured upon first heating was close to that measured in pure MAOP-PDMS shown in Figure 5. However, in the second series of measurements the viscosity of the mixture MAOP-PDMS/HPK notably increased. In the third and successive runs the viscosity variation with temperature did not show any further change. The increase of viscosity of MAOP-PDMS in the presence of the initiator indicates that upon heating partial polymerization of MAOP-PDMS occurred without exposure of the sample to UV irradiation.

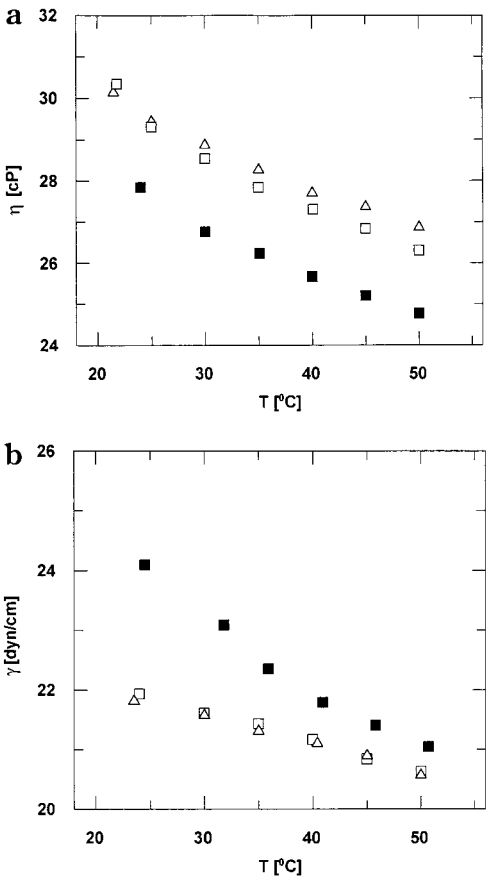

Figure 7. Temperature dependence of viscosity (a) and surface tension (b) of MAOP-PDMS mixed with 1 wt % of HPK: first heating (■), second heating (□), and third heating (△).

The effect of the initiator on the surface tension of MAOP-PDMS was more complicated (Figure 7b). In the temperature range varying from 21 to 50 °C the values of the surface tension obtained in the first measurement were higher than those in the second and third measurements. In addition, the temperature dependence of surface tension on temperature measured in the second and successive heating−cooling cycles became more shallow than that measured in the first run; i.e., $d\gamma/dT$ changed from −0.11 to −0.05 dyn/(cm °C). The change of the surface tension of the mixture MAOP-PDMS/HPK after the first heating−cooling cycle can result from

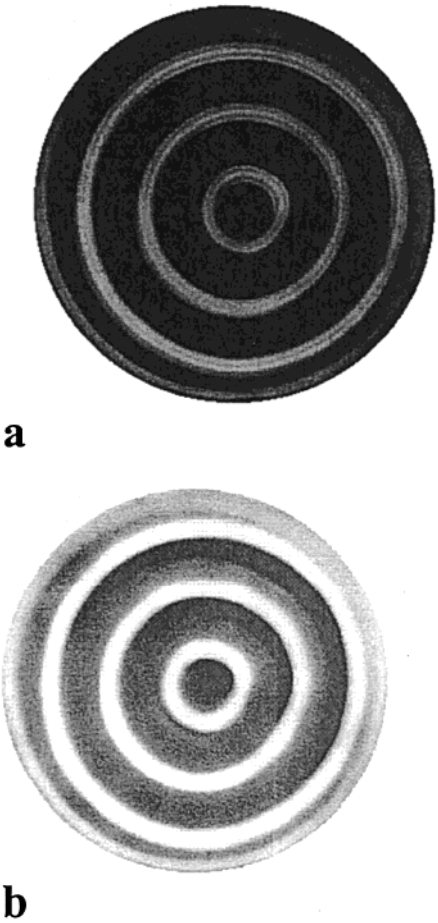

Figure 8. Convection patterns induced in MAOP-PDMS/HPK layer before (a) and following polymerization (b). $d = 0.3096$ cm, $\Delta T = 6.39$ °C.

enrichment of the free fluid surface with the initiator, which may be surface-active, and partial polymerization of MAOP-PDMS upon heating. The contribution of the first effect is, presumably, more significant, which results in a decrease of the surface tension.

The main features of convection in MAOP-PDMS/HPK films were similar to those in pure MAOP-PDMS. The onset of convection in 0.2064 and 0.3096 cm thick films shifted to greater values of ΔT_c than those in MAOP-PDMS (Table 3), a result which is in accord with the decrease in $d\gamma/dT$ and the increase in viscosity caused by partial polymerization of the sample. A typical roll-like convection pattern induced in 0.3096 cm thick MAOP-PDMS films at $\Delta T = 6.39$ °C is shown in Figure 8a. This planform did not change up to $\Delta T = 8.76$ °C. The wavenumber in such patterns was 2.95, i.e., close to $k = 3.02$ measured in MAOP-PDMS. Upon cooling of the MAOP-PDMS/HPK films, some hysteresis was noticed; i.e., the onset of convection shifted to the higher ΔT_c.

UV-induced polymerization of the liquid films with ordered convection patterns was carried out in a delicate way in order to preserve the temperature gradients.[21] The reaction rate has to be such that the change in $d\gamma/dT$, and especially the increase in viscosity of the fluid caused by polymerization, does not lead to the dissipation of the convection patterns. In addition, heating of the sample due to absorption of light should not induce distortions in ordered nonequilibrium structures. Generally, a moderate irradiation time at the reduced intensity of irradiation, and relatively low initiator concentrations, favor conservation of patterns.

Irradiation of the liquid layers of MAOP-PDMS mixed with 1 wt % of HPK for longer than 3 min led to "freezing" of the ordered convection patterns. Figure 8b shows the convection pattern displayed in Figure 8a after polymerization. The roll-like pattern generated in a liquid state retained its main features. The wavenumber slightly increased from 2.95 to 2.98.

In addition to periodic concentric rings generated in the lateral plane of the film, the solid sample featured small periodic vertical deflections of the free surface. Thin rolls corresponding to white rings in Figure 8b were elevated with respect to the wide rolls. The deflection of the free surface in convecting fluid films results from the temperature differences at the liquid−air interface.[8] Depending on the dominant mechanism of convection, the hotter spots are depressed (in surface-tension-driven convection) or elevated (in buoyancy-driven convection). The typical range of vertical surface deflection in fluid layers subjected to convection is on the order of several microns,[22] i.e., significantly smaller than the characteristic lateral length scale. In typical convection experiments with simple fluids, the surface deflection is difficult to study, and it is generally neglected. However, convection-induced surface roughness becomes important (or more specifically, disadvantageous) in polymer coatings cast from polymer solutions. The deflection of the free surface of the coating reduces its decorative properties, such as smoothness and gloss. Polymerization of convecting fluids allows one to explore the effect of convection on the surface topography of the polymeric films and to find effective methods to reduce their surface roughness.

Summary

We showed that in thin films of oligomeric PDMS end-terminated with silanol and aminopropyl groups surface-tension-driven convection is essentially similar to that in pure PDMS. In contrast, in the layers of MAOP-PDMS surface-tension-driven convection is suppressed. This is an unexpected feature since the macroscopic physical properties of MAOP-PDMS favor this type of convection. Undulation patterns can be generated only in relatively thick fluid films of MAOP-PDMS, in which both surface-tension-driven- and buoyancy-driven effects take place. These patterns can be trapped in the solid state by the UV-induced photopolymerization of MAOP-PDMS.

Acknowledgment. The authors gratefully acknowledge the support of the National Science and Engineering Research Centre of Canada and DuPont Canada. E.K. thanks the Ontario Government for a PREA award. We also thank W. Tokaruk and Prof. S. Morris for their assistance in assembling the experimental setup and Prof. A. Mandelis for his help in measuring the thermodiffusivity of MAOP-PDMS.

References and Notes

(1) Moses, E.; Kume, T.; Hashimoto, T. *Phys. Rev. Lett.* **1994**, *72*, 2037−2040.
(2) Trang-Cong, Q.; Harada, A. *Phys. Rev. Lett.* **1996**, *76*, 1162−1165.
(3) Widawski, G.; Rawiso, M.; François, B. *Nature* **1994**, *369*, 387−389.

(4) Mitov, Z.; Kumacheva, E. *Phys. Rev. Lett.* **1998**, *81*, 3427−3430.
(5) (a) Sakurai, S.; Tanaka, K.; Nomura, S. *Polymer* **1993**, *34*, 1089−1092. (b) Sakurai, S.; Tanaka, K.; Nomura, S. *Macromolecules* **1992**, *25*, 7066−7068.
(6) Kumacheva, E.; Li, L.; Winnik, M. A.; Shinozaki, D. M.; Cheng, P. C. *Langmuir* **1997**, *13*, 2483−2489.
(7) Kumaki, J.; Hashimoto, T.; Granick, S. *Phys. Rev. Lett.* **1996**, *77*, 1990−1993.
(8) See e.g.: Normand, C.; Pomeau, Y.; Velarde, M. G. *Rev. Mod. Phys.* **1977**, *49*, 581−624 and references herein.
(9) Pearson, J. R. A. *J. Fluid Mech.* **1958**, *4*, 489−500.
(10) Schatz, M. F.; VanHook, S. J.; McCormick, W. D.; Swift, J. B.; Swinney, H. L. *Phys. Rev. Lett.* **1995**, *75*, 1938−1941.
(11) Nield, D. A. *J. Fluid Mech.* **1964**, *19*, 341−347.
(12) Assenheimer, M.; Khaykovich, B.; Steinberg, V. *Physica A* **1994**, *208*, 373−393.
(13) All experimental parameters are provided by Gelest Inc.
(14) Koschmieder, E. L.; Biggersraff, M. I. *J. Fluid Mech.* **1986**,*167*, 49−64.
(15) *CRC Handbook of Chemistry and Physics*, 59th ed.; CRC Press: West Palm Beach, 1978.
(16) Shen, J.; Mandelis, A. *Rev. Sci. Instrum.* **1995**, *66*, 4999−5005.
(17) It was assumed that thermodiffusivity change with temperature is insignificant and $k = 0.0086$ cm^2/s[15] was used for PDMS, OH-PDMS, and NH_2-PDMS.
(18) For 0.1376 cm thick films of PDMS, OH-PDMS, and NH_2-PDMS Ra_c is 16.2, 11.9, and 15.9, respectively; thus, the buoyancy-driven effects were neglected.
(19) Velarde, M. G.; Perez Cordon, R. *J. Phys. (Paris)* **1976**, *37*, 177−182.
(20) Denn, M. M. *Annu. Rev. Fluid Mech.* **1990**, *22*, 13−34.
(21) Xu, S.; Li, M.; Kumacheva, E. *Langmuir*, in press.
(22) Cerisier, P.; Jamond, C.; Pantaloni, J.; Chermet, J. C. *J. Phys. (Paris)* **1984**, *45*, 405−411.

MA992156T